BIOMOLECULES & THERAPEUTICS

Original Article
Biomol Ther 28(2), 152-162 (2020)

PEGylated Erythropoietin Protects against Brain Injury in the MCAO-Induced Stroke Model by Blocking NF-κB Activation

Jun Hyung Im[1,†], In Jun Yeo[1,†], Chul Ju Hwang[1], Kyung Sun Lee[2] and Jin Tae Hong[1,*]

[1]College of Pharmacy and Medical Research Center, Chungbuk National University, Cheongju 28160,
[2]R&D Center, Ts Corporation, Incheon 22300, Republic of Korea

Abstract

Cerebral ischemia exhibits a multiplicity of pathophysiological mechanisms. During ischemic stroke, the reactive oxygen species (ROS) concentration rises to a peak during reperfusion, possibly underlying neuronal death. Recombinant human erythropoietin (EPO) supplementation is one method of treating neurodegenerative disease by reducing the generation of ROS. We investigated the therapeutic effect of PEGylated EPO (P-EPO) on ischemic stroke. Mice were administered P-EPO (5,000 U/kg) via intravenous injection, and middle cerebral artery occlusion (MCAO) followed by reperfusion was performed to induce *in vivo* ischemic stroke. P-EPO ameliorated MCAO-induced neurological deficit and reduced behavioral disorder and the infarct area. Moreover, lipid peroxidation, expression of inflammatory proteins (cyclooxygenase-2 and inducible nitric oxide synthase), and cytokine levels in blood were reduced by the P-EPO treatment. In addition, higher activation of nuclear factor kappa B (NF-κB) was found in the brain after MCAO, but NF-κB activation was reduced in the P-EPO-injected group. Treatment with the NF-κB inhibitor PS-1145 (5 mg/kg) abolished the P-EPO-induced reduction of infarct volume, neuronal death, neuroinflammation, and oxidative stress. Moreover, P-EPO was more effective than EPO (5,000 U/kg) and similar to a tissue plasminogen activator (10 mg/kg). An *in vitro* study revealed that P-EPO (25, 50, and 100 U/mL) treatment protected against rotenone (100 nM)-induced neuronal loss, neuroinflammation, oxidative stress, and NF-κB activity. These results indicate that the administration of P-EPO exerted neuroprotective effects on cerebral ischemia damage through anti-oxidant and anti-inflammatory properties by inhibiting NF-κB activation.

Key Words: PEGylated erythropoietin, Nuclear factor kappa B, Reactive oxygen species, Stroke, Inflammation

INTRODUCTION

Stroke is reportedly the leading global cause of millions of deaths and disability according to the World Heart Association (2015). Ischemic stroke is the most common form, accounting for 87% of all types of stroke (Bennett *et al*., 2014). Despite its high prevalence, there are no effective treatments currently available. Tissue plasminogen activator (t-PA) is the only FDA-approved drug that is currently available for patients with ischemic stroke (Bonifacio *et al*., 2015). However, it must be administered within 3.5 h of stroke onset, and only a few patients (<3%) can benefit from this therapy (Berrouschot *et al*., 2016). Thus, to find new therapeutic strategies, additional fundamental mechanisms of action should be identified to treat stroke injury. Ischemic stroke events decrease oxygen and glucose delivery to brain tissue (Zamani *et al*., 2013) resulting from the suppression of blood flow to the brain, and can cause metabolic and functional damage (Mestriner *et al*., 2013). Various pathogenic mechanisms contribute to damage during ischemia, including energetic failure (glucose) (Abramov *et al*., 2007) and the generation of free radicals (Allen and Bayraktutan, 2009). Reactive oxygen species (ROS) (Subiros *et al*., 2012) have a well-known critical role in brain damage after brain stroke (Liu *et al*., 2012). Consequently, ROS induce neuronal death by inducing neuroinflammation (Bonda *et al*., 2010; Dumont and Beal, 2011).

Neuronal death following ischemic stroke involves the induction of genes associated with several cellular functions, including apoptosis, inflammation, and oxidative stress. Nuclear factor kappa B (NF-κB) is a transcription factor that is widely known to be associated with inflammatory responses following ischemia and other neuroinflammatory disorders (Simmons *et al*., 2016). Released p65/p50 NF-κB dimers translocate from the cytoplasm to the nucleus where they bind

Open Access **https://doi.org/10.4062/biomolther.2019.147**

Received Sep 9, 2019 **Revised** Oct 12, 2019 **Accepted** Oct 28, 2019
Published Online Dec 9, 2019

***Corresponding Author**
E-mail: jinthong@chungbuk.ac.kr
Tel: +82-43-261-2813, Fax: +82-43-268-2732
[†]The first two authors contributed equally to this work.

to specific DNA sequences and promote the transcription of target genes, such as inducible nitric oxide synthase (iNOS) and cyclooxygenase-2 (COX-2), as well as cytokines. Thus, activation of NF-κB triggers the production of pro-inflammatory cytokines and nitric oxide. In stroke patients, increased protein levels of tumor necrosis factor (TNF)-α signal activation of NF-κB (Jickling *et al*., 2012). Several studies have shown that inhibiting NF-κB results in the suppression of neutrophil recruitment, reduced cytokine release, and oxidative stress in ischemic stroke (Nijboer *et al*., 2008). Acute ischemia inflammatory proteins and cytokines are reduced in p50-knockout mice compared to those in wild-type mice (Duckworth *et al*., 2006; Campbell *et al*., 2008).

Erythropoietin (EPO) is a well-known cytokine that is also produced in the central nervous system, where it exerts neuroprotective actions (Masuda *et al*., 1993; Digicaylioglu *et al*., 1995; Marti, 2004; Jelkmann, 2011). Many compounds that target stroke treatment are effective in animal models but unsuccessfully translated to humans. However, both animal and human clinical studies have shown that EPO might be effective against hypoxic, ischemic, and traumatic brain injuries and both chronic and progressive degenerative disease (Gorio *et al*., 2002; Erbayraktar *et al*., 2003; Brines *et al*., 2004; Gorio *et al*., 2005; Heikal *et al*., 2016). In a recent monocentric proof-of-concept study, recombinant human EPO was shown to be safe and beneficial on clinical outcomes in patients with ischemic stroke. In addition, EPO binds specifically to neuronal EPO receptors where it acts in an anti-apoptotic, antioxidant, anti-inflammatory, neurotrophic, neural stem cell-modulating, and neuroplasticity-enhancing fashion (Subiros *et al*., 2012). However, EPO has a relatively short half-life in the body. The advantage of modification (PEGylation of EPO to create; P-EPO) is its long-term stabilization and half-life (Pasut and Veronese, 2012).

In the present study, we investigated the neuroprotective effects of P-EPO in middle cerebral artery occlusion (MCAO)-induced stroke.

MATERIALS AND METHODS

Reagents and animals

P-EPO was obtained from TS Corporation (Incheon, Korea). 8-week-old male ICR mice were purchased from Samtako BioKorea Co (Osan, Korea). All animal experiments were approved by the Chungbuk National University Institutional Animal Care and Use Committee (IACUC) and were performed in accordance with guidelines approved by the Chungbuk National University for the Care and Use of Laboratory Animals (CBNUA-1088-18-01).

Ischemia surgery

The acclimated 9-week-old ICR mice were anesthetized with 3.5% isoflurane, and then maintained with a gas mixture of 75% N_2O and 25% O_2. The middle cerebral artery was occluded for 1 h using sutures (Doccol Corp, Sharon, MA, USA). The right common carotid artery and the right external carotid artery (ECA) were exposed through a middle neck incision. The ECA was dissected distally, ligated, and coagulated along with the terminal lingual and maxillary artery benches. A minimal incision was made in the ECA stump, at an angle of incidence, with iridectomy scissors. Following the incision, occlusion of the MCA was performed by sutures (0.22 mm). During the occlusion period and postoperative period (1 h after occlusion), the animals were kept on a thermostatically controlled warming plates in order to maintain body temperature at 37°C to prevent hypothermia. Following the occlusion, the clips were removed to restore blood for recirculation. The same surgically operated animals without cerebral artery occlusion served as control animals.

Assessment of neurological deficit score

Neurological deficits were evaluated as reported by Longa *et al* (1989). The findings were scored on a five-point scale: (1) failure to extend the left forepaw, (2) decreased grip strength of forepaw, (3) circling left by pulling the tail, (4) spontaneous circling, and (5) falling down. One point given for each assessment, and then the scores were totaled up. Neurological function assessment was performed by an investigator blind to the experimental groups.

Rota-rod test

The Rota-rod test was performed 1 day after surgery. Mice were placed on a Rota-rod treadmill at a constant speed of 10 rpm for 3 min and the latency to fall was measured. The mice were trained before the experiment to remain on a 25-mm diameter rod rotating at 10 rpm for 120 s. Two or three trials were sufficient for the animals to learn this task.

Morphometric determination of infarct volume

For the detection of the ischemia infarction area of the brain, a cross-sectional infarction area on the surfaces of each brain slice was defined by the 2, 3, 5-triphenyltetrazolium chloride (TTC) staining method. After 1-h reperfusion, the mice received an intracardiac perfusion of 0.9% buffered saline. The brain was then removed and cut into 2-mm serial slices starting 1 mm from the frontal pole. The coronal slices were then immersed in a 2% phosphate-buffered solution for 50 min at 37°C. After TTC staining, the slices were fixed in a 10% phosphate-buffered formalin, and the infarction area was then determined by an image analyzer using the Leica Qwin program (Leica Microsystems Imaging Solution Ltd., Cambridge, UK). The infarct area (mm2) from each 2-mm thick brain slice was determined through an imaging program (Sion Image, Scion Corporation, MD, USA), and then the infarct volume of the whole brain (mm3) was calculated by the sum of all the slice (7 slices in 1 brain) infarct areas' volume×thickness (2 mm). The relative infarction volumes were indicated by the percentage of control brain infarction volume.

Cresyl violet staining

The brains were taken out from the skull and postfixed in 4% paraformaldehyde for 24 h at 4°C. The brains were transferred to 30% sucrose solutions. Subsequently, the brains were cut into 25-μm sections by using cryostat microtome (Leica CM1850; Leica Microsystems, Seoul, Korea). The sections of the brains were thoroughly washed with phosphate-buffered saline (PBS) to remove the excess fixative agent and then transferred to gelatin-coated glass slides and stained with 0.1% cresyl violet (2-5 min) for the purpose of identifying cortical layers and cytoarchitectural features of the isocortical region. After this, the sections were washed in distilled water then dehydrated through ascending grades of ethanol, 50, 70, 90, and 100% ethanol for 2 min in each grade followed by a 10

min immersion in a 1:1 mixture of absolute alcohol and xylene. They were cleared in xylene for 5-10 min and mounted in a mounting medium (Cytoseal™ XYL; Thermo Scientific, Pittsburgh, CA, USA).

Lipid peroxidation

The formation of malonaldehyde, as a lipid peroxidation product in the whole brain homogenate of ipsilateral hemisphere (or left hemisphere of the sham-operated control), was determined using lipid peroxidation assay kit (Cell Biolabs, Inc., San Diego, CA, USA).

Western blot analysis

The brain tissues were homogenized with lysis buffer (PROPREP; iNtRON, Sungnam, Korea; n=8 mice per group) and centrifuged at 2,500×g for 15 min at 4°C. Equal amounts of total protein (40 μg) isolated from brain tissues were resolved on 8 or 10% sodium dodecyl sulfate polyacrylamide gels and then transferred to nitrocellulose membranes (Hybond ECL; Amersham Pharmacia Biotech, Piscataway, NJ, USA). Membranes were incubated at room temperature for 2 h with the following specific antibodies: anti-COX-2, anti-IκB, anti-p-IκB, anti- STAT1, anti-p-STAT1, anti- STAT3, anti-p-STAT3, anti- STAT5, anti-p-STAT5 (Cell Signaling Technology, Inc., Beverly, MA, USA), anti-inducible nitric oxide synthase (iNOS) and anti-Glial fibrillary acidic protein (GFAP) (1:1,000 Novus Biologicals, Inc., Littleton, CO, USA), anti-p50, anti-p65, anti-BAX, anti-cleaved caspase-3, histone H1 (1:1,000; Santa Cruz Biotechnologies, Inc., Santa Cruz, CA, USA), anti-hEPO (1:1,000, R&D systems, Inc., Minneapolis, MN), anti-PEG-2-128, anti-PEG-B47 (1:1,000; Abcam, Cambridge, UK) and anti-β-actin (1:2,500; Sigma, St Louis, MO). Blots were then incubated at room temperature for 2 h with, corresponding peroxidase-conjugated anti-mouse or anti-rabbit antibodies (1:2,000; Santa Cruz Biotechnology, Inc.). Immunoreactive proteins were detected using an enhanced chemiluminescence (ECL) Western blotting detection system. The relative density of the protein bands was scanned densitometrically using My Image (SLB, Seoul, Korea) and quantified by Lab Works 4.0 (UVP, Upland, CA, USA).

Immunohistochemical staining

After being anesthetized with diethyl ether, subgroups of mice were perfused intracardially with 50 mL saline. The brains were taken out from the skull and postfixed in 4% paraformaldehyde for 24 h at 4°C. The brains were transferred to 30% sucrose solutions. Subsequently, brains were cut into 25-μm sections by using cryostat microtome (Leica CM1850; LeicaMicrosystems). After multiple washing in PBS, endogenous peroxidase activity was quenched by incubation of the samples in 3% hydrogen peroxide in PBS for 30 min, followed by a 10-min wash in PBS. The sections were then incubated for 2 h at room temperature with a rabbit/mouse polyclonal antibody against GFAP, iNOS (1:300; Novus Biologicals, Inc.) and a rabbit polyclonal antibody against COX-2, p-STAT3 (Tyr 705) (1:300; Cell Signaling Technology, Inc.). After incubation with the primary antibodies, sections were washed in PBS before being incubated for 1 h at room temperature in the presence of biotinylated goat antirabbit or anti-mouse IgG secondary antibodies (1:1,000; Vector Laboratories, Burlingame, CA, USA). Sections were then washed with PBS and incubated with avidin–peroxidase complex (Vector Laboratories) for 30 min before the immunocomplex was visualized using the chromogen 3,3- diaminobenzidine (Vector Laboratories). Sections were then counterstained with hematoxylin. Finally, sections were dehydrated in ethanol, cleared in xylene, and covered with permount (n=8 mice per group).

Levels of IL-6, IL-1β and TNF-α in serum

The levels of IL-6, IL-1β and TNF-α in the brain were measured by a sandwich enzyme-linked immunosorbent assay (ELISA) according to the instructions of the manufacturer. Briefly, dispensed antigen standards and samples were added to each well of 96-well plates pre-coated with first antibodies. After adding Biotin Conjugate Reagent and Enzyme Conjugate Reagent into each well, the plates were incubated at 37°C for 60 min. The plates were then rinsed five times with distilled water. After chromogenic reaction, a Microtiter plate reader within 30 min measured the absorbance at 405 nm. The IL-6, IL-1β and TNF-α levels in the brain were expressed as picogram of cytokines per milligram of brain.

Cell culture and treatment

Pregnant ICR mice were delivered by DBL Company (Daehan Bio Link, Eumsung, Korea) 48 h before being sacrificed and were placed in a CO_2 chamber in a calm room. On Day 17 embryos were removed from pregnant ICR mice (Daehan Bio Link) under intraperitoneal pentobarbitol (Sigma-Aldrich, St. Louis, MO, USA) anesthesia. The mice were then immediately sacrificed. Cortices were dissected, enzymatically dissociated with papain (10 U/mL, Sigma-Aldrich), then exposed for 5 min in a solution that inactivated papain: DNAse I (Invitrogen, Thermo Fisher Scientific, Waltham, MA, USA) and B27 (Gibco, Thermo Fisher Scientific), diluted in Phosphate Buffer Saline (PBS) 1X with D-glucose (33 mmol/L, Sigma-Aldrich). Cells were dissociated by trituration and filtered through a membrane (70 μm, BD Biosciences, CA, USA). Cells were then purified through a BSA solution (8%, Sigma-Aldrich) diluted in Neurobasal A-25 (Invitrogen, Thermo Fisher Scientific). Dishes, with or without glass coverslips, were coated with poly-D-lysine (0.1 mg/mL, Sigma-Aldrich) 24 h prior to culturing. For each experiment, cortices from 8 to 12 embryos per rat were mixed. Experiments were reproduced 3-8 times. Cultures were grown in Neurobasal (Eurobio, Les Ulis, France) supplemented with B27 (Invitrogen, Thermo Fisher Scientific), 2 mmol/L glutamine, 0.1% penicillin and streptomycin (Gibco, Thermo Fisher Scientific), 250 U/mL amphotericin (Invitrogen, Thermo Fisher Scientific), and 1 mmol/L lactic acid (Sigma-Aldrich) at a density of 6×10^5 cells per cm^2. The percentage of neuronal cells in our culture system was more than 90% judged with cell morphology and immunostaining measurement. Cells were incubated at 37°C and 95% humidity with 5% CO_2. When the cells had reached ~80% confluence, they were then treated with freshly prepared rotenone in DMSO (100 nM final concentration).

Statistical analysis

The data were analyzed using the GraphPad Prism 4 software (GraphPad Software, La Jolla, CA, USA). Data are presented as mean ± SD. Differences in the data were assessed by a one-way analysis of variance (ANOVA). When the p value in the ANOVA test indicated statistical significance, the differences were assessed by the Dunnett's test. A value of $p<0.05$ was considered to be statistically significant.

RESULTS

P-EPO reduces infarct volume and behavioral disorder

The neurological deficit scores were lower in the P-EPO group compared to the MCAO-induced group. Infarction volume was evaluated by triphenyltetrazolium chloride (TTC) staining and was significantly reduced in the P-EPO-treated group 24 h after ischemia/reperfusion compared to the vehicle group. The highest infarct volume (total infarction volume was 28 ± 2%) was induced in MCAO-induced mice after ischemia/reperfusion. Ischemia/reperfusion-induced brain infarction was lower (13 ± 3%) in P-EPO-treated mice (Fig. 1A).

P-EPO-induced improvement in motor function was assessed 24 h after cerebral ischemia. One day before the rota-rod test, all mice were placed on the rota-rod treadmill at 10 rpm for 3 min. The latency before falling after ischemia/reperfusion was significantly lower compared to the vehicle-treated mice (22.3 ± 4.8 s). However, treatment with P-EPO increased latency to 59.3 ± 8.3 s (Fig. 1B).

A neurological deficit score on a 5-point rating scale is commonly used to evaluate neurological function in the MCAO model. Modified- EPO-treated mice exhibited a lower neurological deficit score (3.1 points average) at 24-h ischemia reperfusion compared to MCAO-induced mice (Over control; 0.5 points) (Fig. 1C).

P-EPO suppresses apoptosis in infarction area

We used cresyl violet staining to assess apoptosis in the infarct area. We performed MCAO on the right side of the brain, counted the number of stained cells as indicated by cresyl violet, and compared the left and right sides. The right side had more stained cells than the left side, meaning that ischemic hypoxia, derived by MCAO, induced neuronal death. The number of stained cells in the P-EPO-injected mice brain was 490.22/cm^2 on average, compared to the number (372.64/cm2) in MCAO-induced mice (Fig. 1D). This result indicated that P-EPO suppressed neuronal death in ischemic hypoxia. Western blot data for caspase 3 (a pro-apoptotic protein) expression was also lower in the modified-EPO-treated mice brain compared to the MCAO-induced mice brain (Fig. 1E).

P-EPO reduces glutathione/oxidized glutathione (GSH/GSSG) level, and lipid peroxidation

Ischemic hypoxia induces oxidized lipids by forming high ROS levels. Therefore, we compared lipid oxidation in the MCAO mice brain. The malondialdehyde (MDA) levels in the brain were also higher in the MCAO group (0.6536 nmol/mg), but the levels were also reduced by P-EPO treatment (0.3667 nmol/mg) (Fig. 2A). The ratio of GSH and its oxidized product, GSSG, plays a significant role in determining the prooxidant–antioxidant status. Thus, the ratio of GSH to GSSG was determined. The GSH/GSSG ratio was lower in the P-EPO-treated mice brain (0.01651 μmol/mg) than the MCAO-induced mice

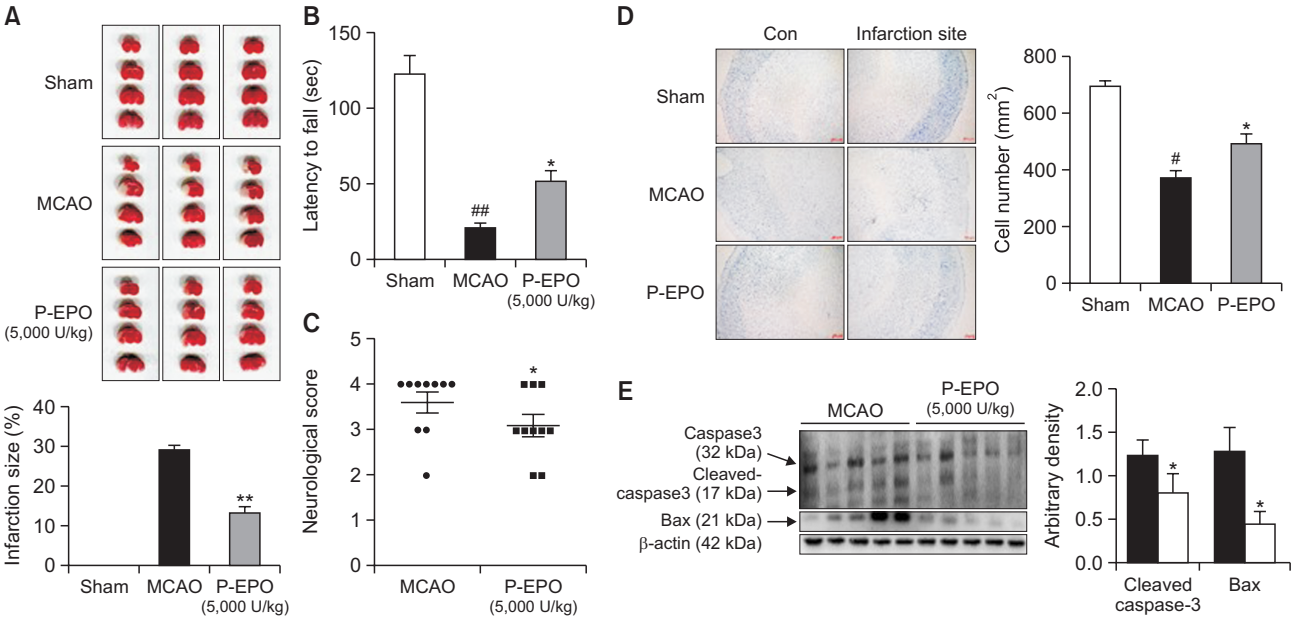

Fig. 1. Effect of P-EPO on ischemia/reperfusion-induced brain infarction and behavior disorder. The test was performed by an investigator blind to the experimental groups and scored by checking the five types of disorder. (A) Brain infarction after ischemia/reperfusion caused by occlusion of bilateral common carotid artery. The brain infarction was detected in brain slices cut 6-mm away from the frontal pole by the 2,3,5-triphenyltetrazolium chloride staining method described in the "Methods" section. The graph represents quantitation of the infarction area. (B) To perform the rota-rod test, the mice were trained on learning day. After 1 day, the retention time on the test stick was recorded. (C) The test was scored by checking the five types of disorder. The scores were then totaled (Sham n=8-9, MCAO n=8-9, M-EPO n=10-12). (D) The brain sections were washed twice with PBS and fixed by incubation in 4 % paraformaldehyde for 1 h at room temperature. Neuronal cells were stained with cresyl violet. The graph represents quantitation of the number of neuronal cells/area (Sham n=3, MCAO n=5, M-EPO n=5). (E) 5,000 U/kg of P-EPO was injected by i.v. before MCAO, and animals from each group were killed 24 h after reperfusion. Activation of caspase 3, Bcl-2, BAX was measured using antibodies against total CCP3, Bcl-2 and BAX. Equal loading of samples was confirmed by monitoring β-actin. Each value is presented as mean ± SD from five mice. *p<0.05, **p<0.01 significant difference from MCAO mice. $^{\#}p$<0.05, $^{\#\#}p$<0.01, significant difference from Sham mice.

brain (0.00453 μmol/mg) (Fig. 2B).

P-EPO reduces neuroinflammatory responses and activation of NF-κB

Activation of astrocytes and microglia is a characteristic feature of neuroinflammation, and these cells promote inflammatory responses when activated. The activation of astrocytes and microglia was identified by immunohistochemistry. The immunohistochemistry results indicated that few cells in the vehicle-treated group were positively stained for GFAP or Iba-1. However, the numbers of GFAP and Iba-1-positive cells were significantly higher in the MCAO group than the vehicle control group, while the numbers of GFAP and Iba-1 cells were significantly lower in the P-EPO-treated groups than the MCAO-induced group. These results suggest that GFAP and Iba-1 were activated by hypoxic ischemia and that P-EPO inhibited the activation of these proteins (Fig. 2C, 2D).

In addition, we compared the expression of GFAP by Western blot in the brains of P-EPO-treated mice and MCAO-induced mice. The results revealed that GFAP levels were significantly lower in the P-EPO-treated brain compared to the MCAO-induced mouse brain (Fig. 3A). The expression of iNOS, COX-2, and Iba-1 was also determined by Western blot. The expression of inflammatory proteins, such as iNOS, COX-2, and Iba-1 in the brains of P-EPO treated mice was much lower than that in MCAO-induced mice. As shown in

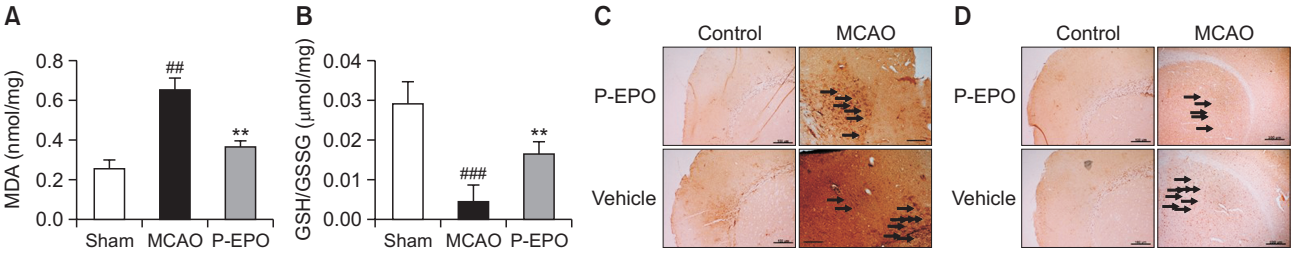

Fig. 2. Effect of P-EPO on MDA and GSH/GSSG levels and expression of GFAP and Iba-1. Vehicle, 5000 U/kg of P-EPO, was administered via i.v. before MCAO. Ischemic brain tissues were processed for immunohistochemistry 24 h after reperfusion following MCAO. (A) MDA levels in the brain infarction site was measured using a TBARS assay kit. (B) GSH/GSSG levels in the brain infarction site were measured using a GSH/GSSG ratio detection assay kit. Representative photomicrographs of (C) GFAP-positive astrocytes, (D) Iba-1-positive microglia/macrophages. Each value is presented as mean ± SD from five mice. $^{**}p<0.01$ significant difference from MCAO mice. $^{\#\#}p<0.01$, $^{\#\#\#}p<0.0001$ significant difference from Sham mice (Sham n=6-7, MCAO n=8-9, M-EPO n=10-12).

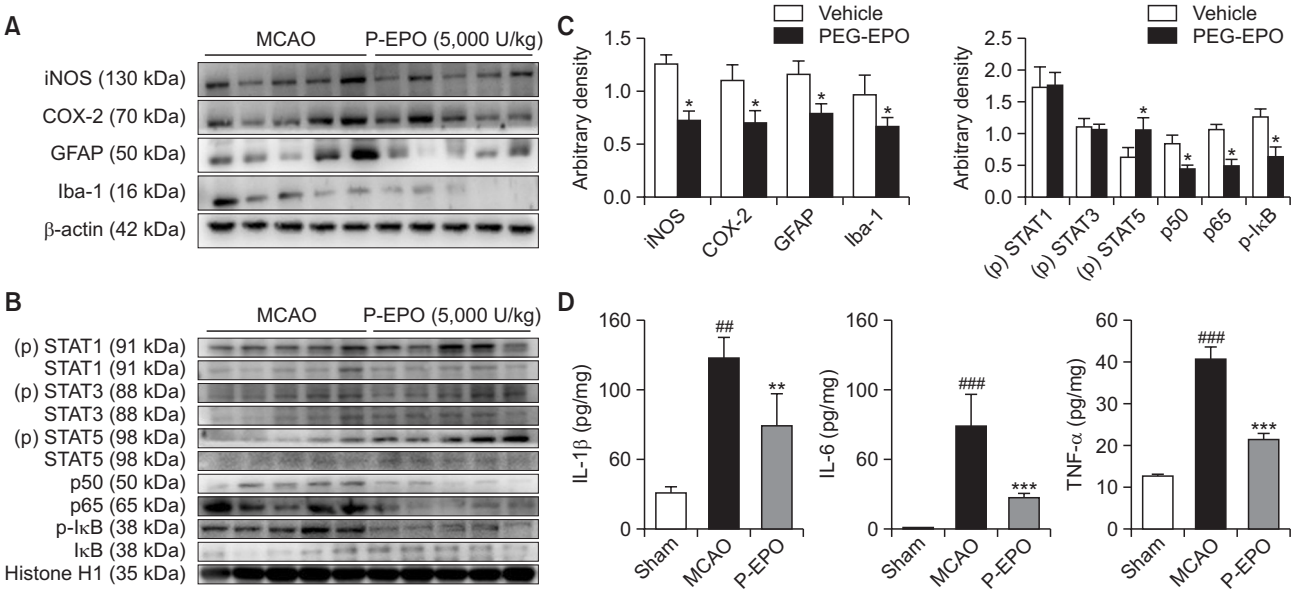

Fig. 3. Effects of P-EPO on inflammatory protein and NF-κB, STAT5 activity. 10 h after reperfusion following 2-h MCAO, vehicle (Sham), 5,000 U/kg of P-EPO was administered via i.v. The ischemic cortex in the striatum was collected for Western blot or immunohistochemistry 24 h after reperfusion following MCAO. (A) Representative Western blots of iNOS, COX-2, GFAP and Iba-1 in the ischemic brain. (B) Representative Western blots of transcription factors STAT1, STAT3, and STAT5 and phosphorylated form and NF-κB factor p50 and p65. Equal loading was confirmed by monitoring the β-actin and histone-H1 protein levels. (C) The expression levels were quantified by stereological analysis using the ImageJ program. (D) Serum levels of cytokines after MCAO measured by ELISA. Anti-inflammatory cytokines (TNF-α, IL-6, IL-1β) were examined. The data are the mean ± SD each sample was probed in triplicate. n=5/group; $^{*}p<0.05$, $^{**}p<0.01$, $^{***}p<0.0001$ significant difference from MCAO mice. $^{\#\#}p<0.01$, $^{\#\#\#}p<0.0001$ significant difference from Sham mice (Sham n=8-9, MCAO n=8-9, M-EPO n=10-12).

Fig. 3A, the expression of inflammatory proteins decreased in response to P-EPO, so we further studied the potential mechanism by which P-EPO inhibited the inflammatory response in the brain. Notably, the P-EPO-treated mouse brain showed significantly lower NF-κB translocation to the nucleus compared to MCAO-induced mice brain (Fig. 3B, 3C).

The pro-inflammatory cytokines TNF-α, IL-6, and IL-1β play important roles in inflammatory disease. Ischemia/reperfusion significantly increases TNF-α and IL-1β levels in the non-transgenic mouse brain. However, TNF-α, IL-1β, and IL-6 release was inhibited in the P-EPO-treated mouse brain (Fig. 3D).

P-EPO reduces ROS and suppresses *in vitro* cell death

Hypoxic ischemia blocks the delivery of oxygen and nutrients to neuron. Rotenone is a specific mitochondrial complex I inhibitor that causes cell damage by generating oxidative stress (Ham and Raju, 2017). Exposure for 24 h to rotenone up to 100 nM causes cell death in a concentration-independent manner in cultured neurons. The MTT assay results revealed that P-EPO significantly increased viability. P-EPO (25, 50, and 100 U/mL) and rotenone increased neuronal viability by 79.6, 83.0, and 89.2%, respectively (Fig. 4A). Whole-cell intracellular ROS production was also quantified as an index of rotenone-induced oxidative stress. Exposure to 100 nM rotenone for 24 h caused a significant increase of H_2O_2, but treatment with P-EPO reduced this (Fig. 4B).

P-EPO reduces activation of NF-κB *in vitro*

NF-κB mediates oxidative stress and inflammatory-induced neuronal death. Thus, we determined the NF-κB DNA binding activity and phosphorylation. We treated neuronal cells with

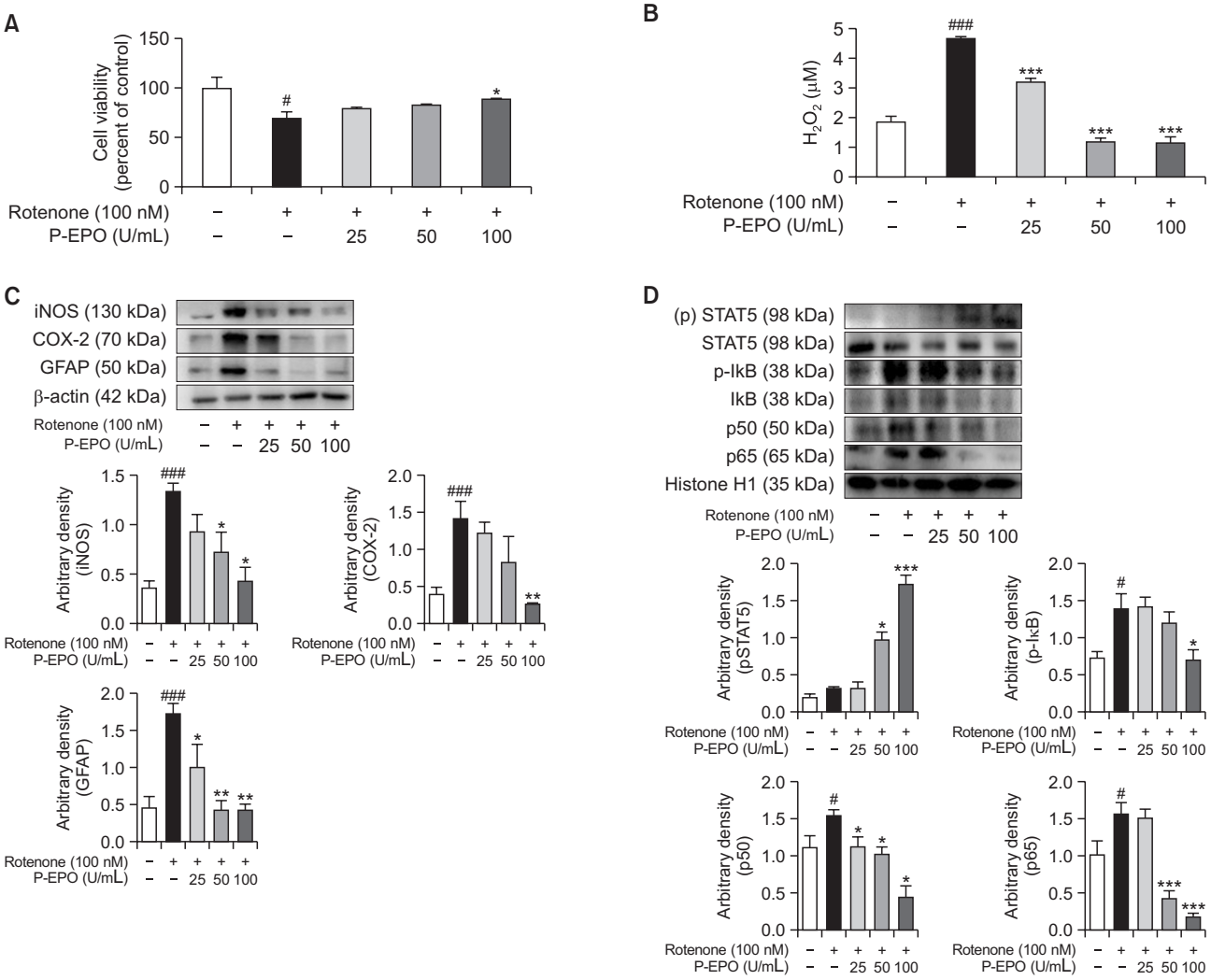

Fig. 4. Effects of EPO on rotenone-induced oxidative stress. Neuronal cells were pretreated for 2 h with P-EPO 25, 50, or 100 U/mL and then incubated with vehicle (control) or the indicated Rotenone at a dose of 100 nM for 24 h. (A) Cell viability was examined by the MTT assay. The results are expressed as a percentage of the control group. (B) H_2O_2 levels in the culture medium were measured using a hyperoxidation assay kit. Representative Western blots are shown in (C, D). Equal loading was confirmed by monitoring the β-actin protein level. The levels of iNOS, COX-2, and GFAP and NF-κB factor p50, p65, p-IκB and STAT5 were quantified by stereological analysis using the ImageJ program. The data are the mean ± SD from three independent experiments (*p<0.05, **p<0.01, ***p<0.0001 significant difference from rotenone group. $^{\#}p$<0.05, $^{\#\#\#}p$<0.0001 significant difference from control group).

100 nM rotenone and P-EPO for 15 min to assess the impact. The Western blot results demonstrated that P-EPO reduced the expression of inflammatory proteins, such as iNOS and COX-2 (Fig. 4C). Oxidative stress caused by rotenone increased NF-κB factor (p50 and p65) expression, but modified-EPO reduced the expression of p50 and p65 (Fig. 4D).

Comparison between P-EPO, t-PA, and EPO

We compared the neuroprotective effects of P-EPO with t-PA, a well-known drug for stroke treatment, and naive EPO. Mice received a single administration of t-PA (10 mg/kg) via intravenous injection (i.v.) immediately after MCAO. P-EPO and EPO (5,000 U/kg each) were injected via i.v. before MCAO. The infarction volume (28 ± 2%) after MCAO decreased significantly in response to the t-PA treatment to 7.8 ± 3%, but it was reduced to 13 ± 3% and 19 ± 5% by P-EPO and EPO, respectively (Fig. 5A). MCAO significantly increased the neurological deficit score (3.6), but the neurological deficit score with P-EPO was an average of 3.1, while those of t-PA and EPO were 2.4 and 3.4, respectively (Fig. 5B). We also compared the NF-κB subunit protein expression levels in each group. P-EPO reduced p50, p65, and p-IκB expression more than t-PA

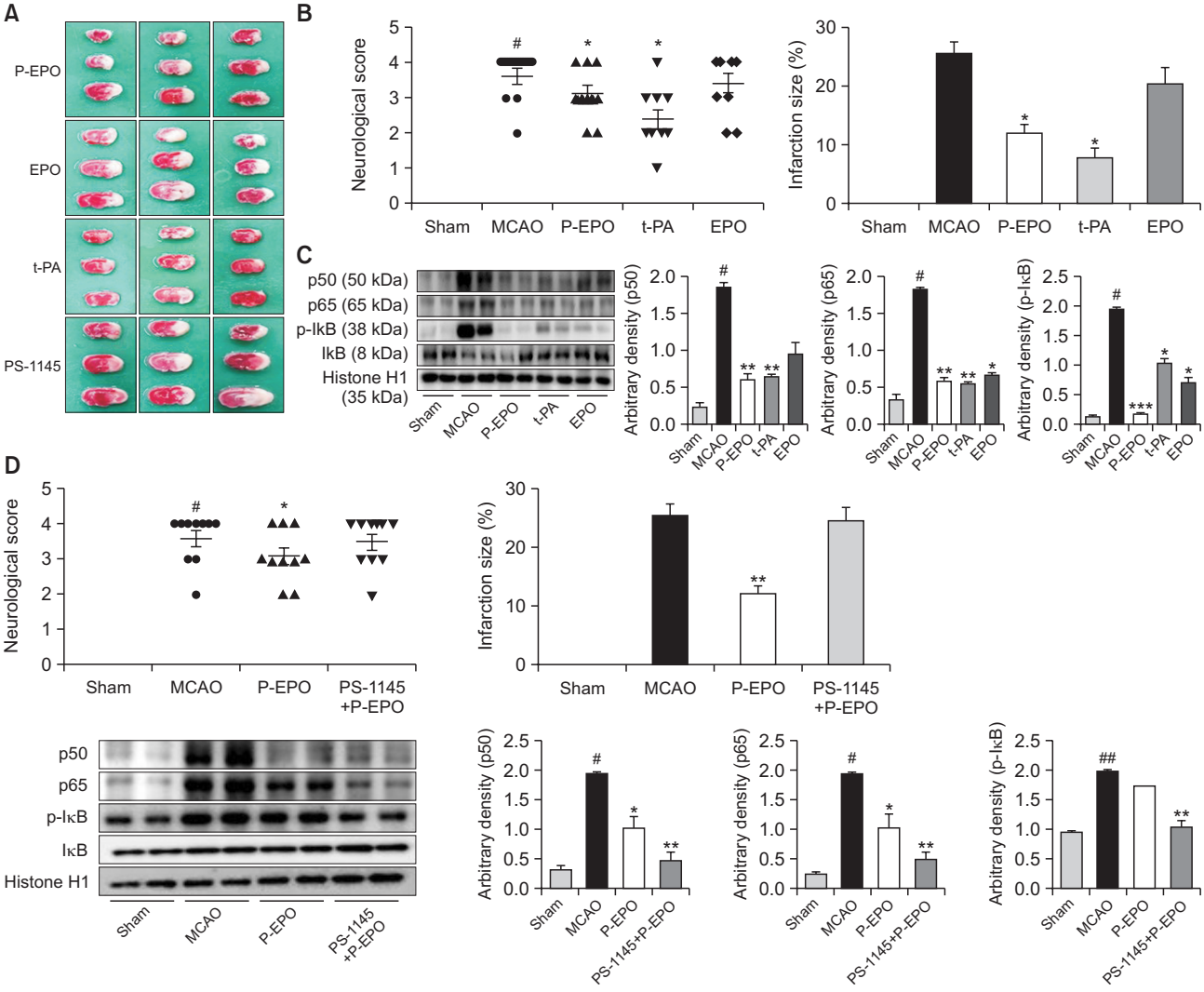

Fig. 5. Effect of P-EPO compared to naive EPO and t-PA and NF-κB inhibitor with P-EPO. P-EPO and naive EPO (5,000 U/kg) were injected via i.v. before MCAO, t-PA (10 mg/kg) was injected via i.v. after MCAO, and PS-1145 (5 mg/kg) was administered via i.p animals from each group were killed 24 h after reperfusion. Brain infarction after ischemia/reperfusion was caused by the occlusion of the bilateral common carotid artery. (A) The brain infarction was detected in brain slices cut 6-mm away from the frontal pole by the 2,3,5-triphenyltetrazolium chloride staining method described in the "Methods" section. The test was scored by checking the five types of disorder. (B, C) The scores were totaled. The graph represents quantitation of the infarction area. Activation of p50, p65, and p-IκB was measured using antibodies against p50, p65, and p-IκB. Equal loading was confirmed by monitoring the histone-H1 protein level. (D) The neurological recovery effect of MCAO by P-EPO was blocked by PS-1145, IκB/IKK inhibitor. The levels of p50, p65, and p-IκB were quantified by stereological analysis using the ImageJ program. The data are the mean ± SD; each sample was probed in triplicate. n=5/group; *p<0.05, **p<0.01, ***p<0.0001 significant difference from MCAO mice. $^{\#}p$<0.05, $^{\#\#}p$<0.01 significant difference from Sham mice (EPO n=10, M-EPO n=10, t-PA n=10, PS-1145 n=10).

and naive EPO (Fig. 5B).

Effects of NF-κB inhibitor and P-EPO combined treatment

To determine whether the effects of P-EPO could be associated with NF-κB during ischemia/reperfusion, we gave mice a single administration of PS-1145 (5 mg/kg) via intraperitoneal injection (i.p.) and modified- EPO (5,000 U/kg) (5 min after PS-1145 treatment) via i.v. before MCAO surgery. Compared to the P-EPO group (12.0 ± 3%), the PS-1145 with P-EPO combination treatment group (24.5 ± 5%) experienced increased infarction volume. The neurological deficit score in the PS-1145 and P-EPO combination treated group was 3.5 on average, but that of P-EPO was 3.1 (Fig. 5C). We also detected a combination effect of PS-1145 and P-EPO; however, unexpectedly reduced p50, p65, and p-IκB expression by P-EPO was not reversed by PS-1145 (Fig. 5D).

DISCUSSION

This study shows for the first time that P-EPO therapy attenuates brain damage and behavioral dysfunction caused by MCAO, resulting in improved behavioral functioning. The improved functional performance is correlated with reduced infarction volume after MCAO. Many researchers have become interested in the non-hematopoietic functions of EPO, particularly the protection of cells in various organs (such as the brain, retina, heart, and kidneys) against ischemic injury (Grasso *et al*., 2004; van Rijt *et al*., 2014). Yoo *et al*. (2017) reported an approximately 25% neuroprotective effect from a single treatment of EPO (3,000 U/kg) in a rat stroke model. Another study reported that treating mice with EPO (5,000 U/kg) for 11 days (five injections) after MCAO reduced infarction volume by about 50% (Wang *et al*., 2017). In other research, a single treatment of EPO (5,000 U/kg) after MCAO was found to reduce the infarction size by 50% in a rat model (Mrsic-Pelcic *et al*., 2017). However, our study showed an 87% reduction in infarction volume after administering P-EPO. In addition, modified- EPO (3.1) resulted in a lower neurological deficit score than EPO (3.5) after MCAO (Wang *et al*., 2017). Another study indicated that EPO (5,000 U/kg) treatment reduced the MDA level by 14% in a rat renal ischemia/reperfusion model (Ahmadiasl *et al*., 2013), whereas P-EPO reduced the MDA level by 43% in the present study. P-EPO is manufactured by the covalent conjugation of PEG and EPO to prolong its half-life in the human body. Generally, protein drugs have several issues, such as rapid clearance, structural instability, and immunogenicity. The half-life of naive EPO is 8 h, whereas that of P-EPO is 24 h. Moreover, PEGylated proteins have structural stability and no immunogenicity (Abed *et al*., 2017). In the present study, P-EPO had a significant protective effect on MCAO-induced brain damage in mice, and P-EPO was more effective than naive EPO and thus comparable to t-PA. Therefore, P-EPO could be a more suitable treatment for stroke.

Oxidative stress is considered the primary event during MCAO because ischemia/reperfusion stimulates overproduction of ROS, such as hydrogen peroxide (H_2O_2), which leads to the oxidation of proteins, lipids, and DNA and possibly cell death (Hosoo *et al*., 2017). Antioxidant enzymes, such as GSH, protect against oxidative stress; these compounds play a crucial role in protecting neurons against ROS-induced cell death (Wang *et al*., 2013). MCAO-operated rats exhibit increased MDA and decreased GSH levels (Zhang *et al*., 2017a; Wang *et al*., 2018), but treatment with EPO reduces MDA and increases GSH in rats with spinal-cord trauma (Yazihan *et al*., 2008). Moreover, EPO (2,500 U/day) reduces MDA levels in Parkinson's rats (Erbas *et al*., 2015). Other studies have reported a decrease of lipid peroxidation in brain samples from Alzheimer's disease animals treated with EPO (Chen *et al*., 2015). EPO has an anti-oxidant effect in human samples that reduces HO• levels by directly scavenging HO• at a diffusion-controlled rate and further suppressing the Fenton formation of HO• through catalytic iron chelation (Bailey *et al*., 2014). In the present study, the GSH/GSSG ratio and MDA content decreased significantly with P-EPO treatment after MCAO. Furthermore, P-EPO reduced rotenone-induced H_2O_2 concentrations in neuronal cells. These results indicate that the antioxidant property of P-EPO could result in a neuroprotective effect against MCAO.

MCAO also initiates neuroinflammation by producing inflammatory cytokines, such as IL-1β, TNF-α, and IL-6, thereby aggravating brain damage (Kraft and Harry, 2011). A high concentration of TNF-α has a direct toxic effect on neurons. TNF-α transgenic mice develop severe inflammation and exhibit brain and neurodegenerative diseases (Gong *et al*., 2014) and IL-6 accelerates the pathological processes of central nervous system disorders (Zhang *et al*., 2017b). Another study indicated that COX-2 and iNOS levels increase significantly in the cerebral cortex after MCAO, but EPO treatment reduces their expression (Gui *et al*., 2015; Wang *et al*., 2015; Hu *et al*., 2016). Moreover, it has been demonstrated that EPO protects the brain through an anti-inflammatory mechanism that reduces TNF-α, and IL-6 in hemorrhagic shocked rats (Ranjbaran *et al*., 2017). Many other neurodegenerative experimental models have demonstrated that EPO reduces neuroinflammation. EPO is associated with prevention of the development of Alzheimer's disease by reducing neuroinflammatory cytokines, such as IL-10, IL-8, and TNF-α (Kim *et al*., 2011). EPO also reduces iNOS gene expression in a peripheral neurotoxicity model and TNF-α levels in a Parkinson's model (Erbas *et al*., 2015; Sharawy *et al*., 2015). Other studies have shown that EPO significantly reduces TNF-α levels and neuronal loss in an Alzheimer's model (Cevik *et al*., 2017). EPO attenuates Aβ42-induced memory deficits and efficiently arrests tau hyperphosphorylation by inhibiting glycogen synthase kinase 3 beta activity in mice (Li *et al*., 2015). In this study, we demonstrated that COX-2, iNOS, TNF-α, IL-1β, and IL-6 increased in response to MCAO, but treatment with P-EPO reduced their levels. Moreover, rotenone increased iNOS, COX-2, and GFAP expression in neuronal cells, whereas P-EPO reduced their expression. Consequently, these anti-inflammatory effects of modified-EPO could be associated with its neuroprotective effects against MCAO.

NF-κB is an important transcription factor involved in the expression of inflammatory genes including iNOS and COX2; therefore, it regulates inflammatory responses (Qin *et al*., 2017). It has also been demonstrated that inhibiting NF-κB suppresses local inflammation after cerebral ischemia, which contributes to neuroprotection (Zhu *et al*., 2012). Acute brain injury induced by intracerebral injection of IL-1 provokes rapid activation of brain NF-κB. NF-κB knockout mice, which lack anti-inflammatory p50, have smaller brain infarction volume, which is associated with increased neutrophil recruitment to the brain, compared to wild-type mice. Another study also

showed that ischemia/reperfusion damage is significantly reduced in p50 knockout compared to wild-type mice (Campbell *et al*., 2008). Moreover, ischemia-induced brain damage in rats was significantly elevated by stimulating the NF-κB-mediated inflammatory responses (Crack *et al*., 2006). Reportedly, EPO protects neurons from hypoxic injury by modulating Toll-like receptor-mediated inflammatory responses (Rocchetta *et al*., 2011). Research has also shown that EPO decreases brain carbon monoxide poisoning-induced cerebral injury by inhibiting activation of NF-κB (Pang *et al*., 2016). In this study, we demonstrated that P-EPO exerted a neuroprotective role by reducing NF-κB activity. Moreover, treating P-EPO with an NF-κB inhibitor (PS-1145, 10 mg/kg) reversed the effects of P-EPO on infarction volume and neurological deficit score in MCAO mice. In addition, expression of NF-κB regulatory pro-apoptotic target proteins, such as Bax and caspase-3, decreased greatly in the MCAO-injured brain of P-EPO injected mice compared to the MCAO group. In an *in vitro* study, rotenone induced H_2O_2, and increased cell viability. Furthermore, p50, p65 and p-IκB were increased by rotenone, but P-EPO reduced their expression. These data indicate that blocking of NF-κB pathway obstructed the P-EPO-mediated NF-κB signal pathway, which resulted in blocking of the P-EPO action mechanism. We also detected a combination effect of PS-1145 and P-EPO. However, inconsistent with the effect on infarction volume and neurological score, reduced p50, p65, and p-IκB expression by P-EPO was not reversed by PS-1145 (Fig. 5D). These data suggest that blocking of NF-κB signals as well as other signals could be involved in the effect of P-EPO in stroke development. Thus, our data indicate that the lowered activation of NF-κB by P-EPO could be a partially protective mechanism of P-EPO in MCAO-induced brain injury.

In this study, EPO and P-EPO crossed the blood–brain barrier (BBB) (Supplementary Fig. 1), and P-EPO had a greater therapeutic effect than EPO in the MCAO model, but a similar protective effect to t-PA. However, unlike t-PA, which was administered after MCAO, P-EPO was administered before MCAO. t-PA has a short half-life of around 5-10 min in circulation and crosses both the intact and damaged BBB into ischemic brain tissue; thus, t-PA may exert a neurotoxic effect and could damage other tissues (Liu *et al*., 2018). Modified-EPO has a longer half-life (24 h) but may not be toxic to other tissues. Moreover, the protective effect of P-EPO indicated that it could be applicable for preventing stroke. Taken together, the present study indicates that P-EPO could be suitable for preventing stroke, and that P-EPO is more effective than EPO.

CONFLICT OF INTEREST

The authors declare no conflicts of interest.

ACKNOWLEDGMENTS

This work was supported by the National Research Foundation of Korea (NRF) grant funded by the Korea government (MSIP) (NO. MRC2017R, A5A2015541) and by a research grant funded by Ts Corporation of Korea.

REFERENCES

Abed, H. S., Al-Ghobashy, M. A., Fathalla, F. A. and Salem, M. Y. (2017) Evaluation of the combined effects of pegylation and glycosylation on the stability of erythropoietin using a stability-indicating SE-HPLC. *Biologicals* **50**, 129-136.

Abramov, A. Y., Scorziello, A. and Duchen, M. R. (2007) Three distinct mechanisms generate oxygen free radicals in neurons and contribute to cell death during anoxia and reoxygenation. *J. Neurosci.* **27**, 1129-1138.

Ahmadiasl, N., Banaei, S. and Alihemmati, A. (2013) Combination antioxidant effect of erythropoietin and melatonin on renal ischemia-reperfusion injury in rats. *Iran. J. Basic Med. Sci.* **16**, 1209-1216.

Allen, C. L. and Bayraktutan, U. (2009) Oxidative stress and its role in the pathogenesis of ischaemic stroke. *Int. J. Stroke* **4**, 461-470.

Bailey, D. M., Lundby, C., Berg, R. M., Taudorf, S., Rahmouni, H., Gutowski, M., Mulholland, C. W., Sullivan, J. L., Swenson, E. R., McEneny, J., Young, I. S., Pedersen, B. K., Moller, K., Pietri, S. and Culcasi, M. (2014) On the antioxidant properties of erythropoietin and its association with the oxidative-nitrosative stress response to hypoxia in humans. *Acta Physiol. (Oxf.)* **212**, 175-187.

Bennett, D. A., Krishnamurthi, R. V., Barker-Collo, S., Forouzanfar, M. H., Naghavi, M., Connor, M., Lawes, C. M., Moran, A. E., Anderson, L. M. and Roth, G. A. (2014) The global burden of ischemic stroke: findings of the GBD 2010 study. *Global Heart* **9**, 107-112.

Berrouschot, J., Stoll, A., Hogh, T. and Eschenfelder, C. C. (2016) Intravenous thrombolysis with recombinant tissue-type plasminogen activator in a stroke patient receiving dabigatran anticoagulant after antagonization with idarucizumab. *Stroke* **47**, 1936-1938.

Bonda, D. J., Wang, X., Perry, G., Nunomura, A., Tabaton, M., Zhu, X. and Smith, M. A. (2010) Oxidative stress in Alzheimer disease: a possibility for prevention. *Neuropharmacology* **59**, 290-294.

Bonifacio, E., Ziegler, A. G., Klingensmith, G., Schober, E., Bingley, P. J., Rottenkolber, M., Theil, A., Eugster, A., Puff, R., Peplow, C., Buettner, F., Lange, K., Hasford, J. and Achenbach, P.; Pre-POINT Study Group (2015) Effects of high-dose oral insulin on immune responses in children at high risk for type 1 diabetes: the Pre-POINT randomized clinical trial. *JAMA* **313**, 1541-1549.

Brines, M., Grasso, G., Fiordaliso, F., Sfacteria, A., Ghezzi, P., Fratelli, M., Latini, R., Xie, Q. W., Smart, J., Su-Rick, C. J., Pobre, E., Diaz, D., Gomez, D., Hand, C., Coleman, T. and Cerami, A. (2004) Erythropoietin mediates tissue protection through an erythropoietin and common beta-subunit heteroreceptor. *Proc. Natl. Acad. Sci. U.S.A.* **101**, 14907-14912.

Campbell, S. J., Anthony, D. C., Oakley, F., Carlsen, H., Elsharkawy, A. M., Blomhoff, R. and Mann, D. A. (2008) Hepatic nuclear factor kappa B regulates neutrophil recruitment to the injured brain. *J. Neuropathol. Exp. Neurol.* **67**, 223-230.

Cevik, B., Solmaz, V., Yigitturk, G., Cavusoglu, T., Peker, G. and Erbas, O. (2017) Neuroprotective effects of erythropoietin on Alzheimer's dementia model in rats. *Adv. Clin. Exp. Med.* **26**, 23-29.

Chen, J., Yang, Z. and Zhang, X. (2015) Carbamylated erythropoietin: a prospective drug candidate for neuroprotection. *Biochem. Insights* **8**, 25-29.

Crack, P. J., Taylor, J. M., Ali, U., Mansell, A. and Hertzog, P. J. (2006) Potential contribution of NF-kappaB in neuronal cell death in the glutathione peroxidase-1 knockout mouse in response to ischemia-reperfusion injury. *Stroke* **37**, 1533-1538.

Digicaylioglu, M., Bichet, S., Marti, H. H., Wenger, R. H., Rivas, L. A., Bauer, C. and Gassmann, M. (1995) Localization of specific erythropoietin binding sites in defined areas of the mouse brain. *Proc. Natl. Acad. Sci. U.S.A.* **92**, 3717-3720.

Duckworth, E. A., Butler, T., Collier, L., Collier, S. and Pennypacker, K. R. (2006) NF-kappaB protects neurons from ischemic injury after middle cerebral artery occlusion in mice. *Brain Res.* **1088**, 167-175.

Dumont, M. and Beal, M. F. (2011) Neuroprotective strategies involving ROS in Alzheimer disease. *Free Radic. Biol. Med.* **51**, 1014-1026.

Erbas, O., Cinar, B. P., Solmaz, V., Cavusoglu, T. and Ates, U. (2015) The neuroprotective effect of erythropoietin on experimental Parkinson model in rats. *Neuropeptides* **49**, 1-5.

Erbayraktar, S., Yilmaz, O., Gokmen, N. and Brines, M. (2003) Erythropoietin is a multifunctional tissue-protective cytokine. *Curr. He-*

matol. Rep. **2**, 465-470.
Gong, G., Xiang, L., Yuan, L., Hu, L., Wu, W., Cai, L., Yin, L. and Dong, H. (2014) Protective effect of glycyrrhizin, a direct HMGB1 inhibitor, on focal cerebral ischemia/reperfusion-induced inflammation, oxidative stress, and apoptosis in rats. *PLoS ONE* **9**, e89450.
Gorio, A., Gokmen, N., Erbayraktar, S., Yilmaz, O., Madaschi, L., Cichetti, C., Di Giulio, A. M., Vardar, E., Cerami, A. and Brines, M. (2002) Recombinant human erythropoietin counteracts secondary injury and markedly enhances neurological recovery from experimental spinal cord trauma. *Proc. Natl. Acad. Sci. U.S.A.* **99**, 9450-9455.
Gorio, A., Madaschi, L., Di Stefano, B., Carelli, S., Di Giulio, A. M., De Biasi, S., Coleman, T., Cerami, A. and Brines, M. (2005) Methylprednisolone neutralizes the beneficial effects of erythropoietin in experimental spinal cord injury. *Proc. Natl. Acad. Sci. U.S.A.* **102**, 16379-16384.
Grasso, G., Sfacteria, A., Cerami, A. and Brines, M. (2004) Erythropoietin as a tissue-protective cytokine in brain injury: what do we know and where do we go? *Neuroscientist* **10**, 93-98.
Gui, D., Li, Y., Chen, X., Gao, D., Yang, Y. and Li, X. (2015) HIF1 signaling pathway involving iNOS, COX2 and caspase9 mediates the neuroprotection provided by erythropoietin in the retina of chronic ocular hypertension rats. *Mol. Med. Rep.* **11**, 1490-1496.
Ham, P. B., 3rd and Raju, R. (2017) Mitochondrial function in hypoxic ischemic injury and influence of aging. *Prog. Neurobiol.* **157**, 92-116.
Heikal, L., Ghezzi, P., Mengozzi, M., Stelmaszczuk, B., Feelisch, M. and Ferns, G. A. (2016) Erythropoietin and a nonerythropoietic peptide analog promote aortic endothelial cell repair under hypoxic conditions: role of nitric oxide. *Hypoxia* **4**, 121-133.
Hosoo, H., Marushima, A., Nagasaki, Y., Hirayama, A., Ito, H., Puentes, S., Mujagic, A., Tsurushima, H., Tsuruta, W., Suzuki, K., Matsui, H., Matsumaru, Y., Yamamoto, T. and Matsumura, A. (2017) Neurovascular unit protection from cerebral ischemia-reperfusion injury by radical-containing nanoparticles in mice. *Stroke* **48**, 2238-2247.
Hu, H., Zhu, X., Lin, R., Li, Z. and Chen, L. (2016) Suppressive effects of Gua Lou Gui Zhi decoction on MCAO-induced NO and PGE2 production are dependent on the MAPK and NF-kappaB signaling pathways. *Mol. Med. Rep.* **14**, 5141-5147.
Jelkmann, W. (2011) Regulation of erythropoietin production. *J. Physiol.* **589**, 1251-1258.
Jickling, G. C., Zhan, X., Stamova, B., Ander, B. P., Tian, Y., Liu, D., Sison, S. M., Verro, P., Johnston, S. C. and Sharp, F. R. (2012) Ischemic transient neurological events identified by immune response to cerebral ischemia. *Stroke* **43**, 1006-1012.
Kim, S. M., Song, J., Kim, S., Han, C., Park, M. H., Koh, Y., Jo, S. A. and Kim, Y. Y. (2011) Identification of peripheral inflammatory markers between normal control and Alzheimer's disease. *BMC Neurol.* **11**, 51.
Kraft, A. D. and Harry, G. J. (2011) Features of microglia and neuroinflammation relevant to environmental exposure and neurotoxicity. *Int. J. Environ. Res. Public Health* **8**, 2980-3018.
Li, Y. P., Yang, G. J., Jin, L., Yang, H. M., Chen, J., Chai, G. S. and Wang, L. (2015) Erythropoietin attenuates Alzheimer-like memory impairments and pathological changes induced by amyloid beta42 in mice. *Brain Res.* **1618**, 159-167.
Liu, C., Weaver, J. and Liu, K. J. (2012) Rapid conditioning with oxygen oscillation: neuroprotection by intermittent normobaric hyperoxia after transient focal cerebral ischemia in rats. *Stroke* **43**, 220-226.
Liu, S., Feng, X., Jin, R. and Li, G. (2018) Tissue plasminogen activator-based nanothrombolysis for ischemic stroke. *Expert Opin. Drug Deliv.* **15**, 173-184.
Longa, E. Z., Weinstein, P. R., Carlson, S. and Cummins, R. (1989) Reversible middle cerebral artery occlusion without craniectomy in rats. *Stroke* **20**, 84-91.
Marti, H. H. (2004) Erythropoietin and the hypoxic brain. *J .Exp. Biol.* **207**, 3233-3242.
Masuda, S., Nagao, M., Takahata, K., Konishi, Y., Gallyas, F., Jr., Tabira, T. and Sasaki, R. (1993) Functional erythropoietin receptor of the cells with neural characteristics. Comparison with receptor properties of erythroid cells. *J. Biol. Chem.* **268**, 11208-11216.
Mestriner, R. G., Miguel, P. M., Bagatini, P. B., Saur, L., Boisserand, L. S., Baptista, P. P., Xavier, L. L. and Netto, C. A. (2013) Behavior outcome after ischemic and hemorrhagic stroke, with similar brain damage, in rats. *Behav. Brain Res.* **244**, 82-89.
Mrsic-Pelcic, J., Pilipovic, K., Pelcic, G., Vitezic, D. and Zupan, G. (2017) Decrease in oxidative stress parameters after post-ischaemic recombinant human erythropoietin administration in the hippocampus of rats exposed to focal cerebral ischaemia. *Basic Clin. Pharmacol. Toxicol.* **121**, 453-464.
Nijboer, C. H., Heijnen, C. J., Groenendaal, F., May, M. J., van Bel, F. and Kavelaars, A. (2008) A dual role of the NF-kappaB pathway in neonatal hypoxic-ischemic brain damage. *Stroke* **39**, 2578-2586.
Pang, L., Zhang, N., Dong, N., Wang, D. W., Xu, D. H., Zhang, P. and Meng, X. W. (2016) Erythropoietin protects rat brain injury from carbon monoxide poisoning by inhibiting toll-like receptor 4/NF-kappa B-dependent inflammatory responses. *Inflammation* **39**, 561-568.
Pasut, G. and Veronese, F. M. (2012) State of the art in PEGylation: the great versatility achieved after forty years of research. *J. Control. Release* **161**, 461-472.
Qin, Y. Y., Li, M., Feng, X., Wang, J., Cao, L., Shen, X. K., Chen, J., Sun, M., Sheng, R., Han, F. and Qin, Z. H. (2017) Combined NADPH and the NOX inhibitor apocynin provides greater anti-inflammatory and neuroprotective effects in a mouse model of stroke. *Free Radic. Biol. Med.* **104**, 333-345.
Ranjbaran, M., Kadkhodaee, M. and Seifi, B. (2017) Renal tissue pro-inflammatory gene expression is reduced by erythropoietin in rats subjected to hemorrhagic shock. *J. Nephropathol.* **6**, 69-73.
Rocchetta, F., Solini, S., Mister, M., Mele, C., Cassis, P., Noris, M., Remuzzi, G. and Aiello, S. (2011) Erythropoietin enhances immunostimulatory properties of immature dendritic cells. *Clin. Exp. Immunol.* **165**, 202-210.
Sharawy, N., Rashed, L. and Youakim, M. F. (2015) Evaluation of multi-neuroprotective effects of erythropoietin using cisplatin induced peripheral neurotoxicity model. *Exp. Toxicol. Pathol.* **67**, 315-322.
Simmons, L. J., Surles-Zeigler, M. C., Li, Y., Ford, G. D., Newman, G. D. and Ford, B. D. (2016) Regulation of inflammatory responses by neuregulin-1 in brain ischemia and microglial cells *in vitro* involves the NF-kappa B pathway. *J. Neuroinflammation* **13**, 237.
Subiros, N., Del Barco, D. G. and Coro-Antich, R. M. (2012) Erythropoietin: still on the neuroprotection road. *Ther. Adv. Neurol. Disord.* **5**, 161-173.
van Rijt, W. G., van Goor, H., Ploeg, R. J. and Leuvenink, H. G. (2014) Erythropoietin-mediated protection in kidney transplantation: non-erythropoietic EPO derivatives improve function without increasing risk of cardiovascular events. *Transpl. Int.* **27**, 241-248.
Wang, F. J., Wang, S. X., Chai, L. J., Zhang, Y., Guo, H. and Hu, L. M. (2018) Xueshuantong injection (lyophilized) combined with salvianolate lyophilized injection protects against focal cerebral ischemia/reperfusion injury in rats through attenuation of oxidative stress. *Acta Pharmacol. Sin.* **39**, 998-1011.
Wang, R., Li, J., Duan, Y., Tao, Z., Zhao, H. and Luo, Y. (2017) Effects of erythropoietin on gliogenesis during cerebral ischemic/reperfusion recovery in adult mice. *Aging Dis.* **8**, 410-419.
Wang, T., Zhai, L., Zhang, H., Zhao, L. and Guo, Y. (2015) Picroside II inhibits the MEK-ERK1/2-COX2 signal pathway to prevent cerebral ischemic injury in rats. *J. Mol. Neurosci.* **57**, 335-351.
Wang, T. F., Lei, Z., Li, Y. X., Wang, Y. S., Wang, J., Wang, S. J., Hao, Y. J., Zhou, R., Jin, S. J., Du, J., Li, J., Sun, T. and Yu, J. Q. (2013) Oxysophoridine protects against focal cerebral ischemic injury by inhibiting oxidative stress and apoptosis in mice. *Neurochem. Res.* **38**, 2408-2417.
Yazihan, N., Uzuner, K., Salman, B., Vural, M., Koken, T. and Arslantas, A. (2008) Erythropoietin improves oxidative stress following spinal cord trauma in rats. *Injury* **39**, 1408-1413.
Yoo, S. J., Cho, B., Lee, D., Son, G., Lee, Y. B., Soo Han, H., Kim, E., Moon, C. and Moon, C. (2017) The erythropoietin-derived peptide MK-X and erythropoietin have neuroprotective effects against ischemic brain damage. *Cell Death Dis.* **8**, e3003.
Zamani, M., Katebi, M., Mehdizadeh, M., Kafami, L. and Soleimani, M. (2013) Combination therapy with A1 receptor agonist and vitamin C improved working memory in a mouse model of global ischemia-reperfusion. *Basic Clin. Neurosci.* **4**, 111-116.
Zhang, R. Q., Li, D. Y., Xu, T. D., Zhu, S. S., Pan, H. J., Fang, F., Wu,

X. and Sun, H. (2017a) Antioxidative effect of luteolin pretreatment on simulated ischemia/reperfusion injury in cardiomyocyte and perfused rat heart. *Chin. J. Integr. Med.* **23**, 518-527.

Zhang, Y., Yan, Y., Cao, Y., Yang, Y., Zhao, Q., Jing, R., Hu, J. and Bao, J. (2017b) Potential therapeutic and protective effect of curcumin against stroke in the male albino stroke-induced model rats. *Life Sci.* **183**, 45-49.

Zhu, J., Jiang, Y., Wu, L., Lu, T., Xu, G. and Liu, X. (2012) Suppression of local inflammation contributes to the neuroprotective effect of ginsenoside Rb1 in rats with cerebral ischemia. *Neuroscience* **202**, 342-351.